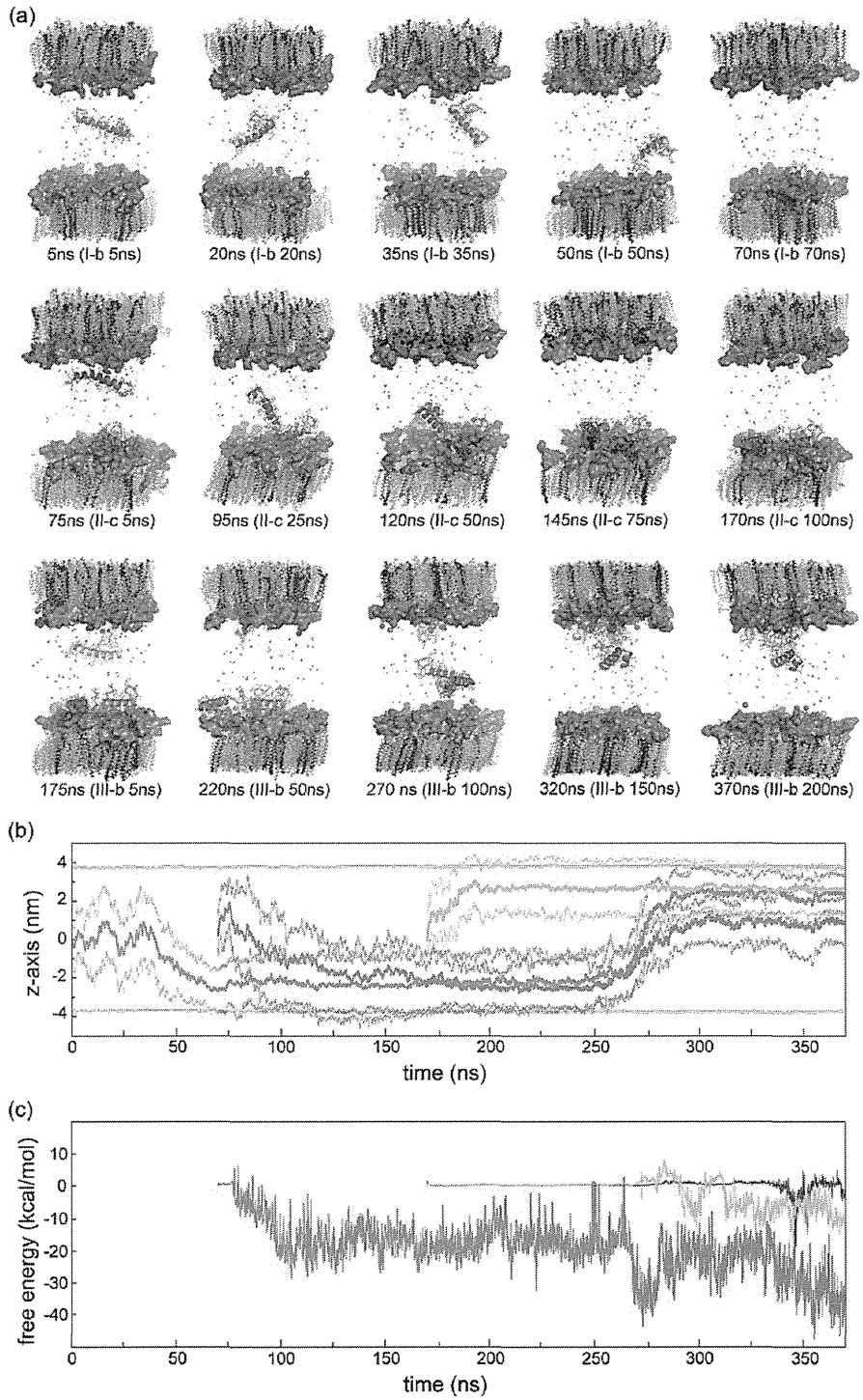

Figure 2. (a) Motion of the Aβ peptide. Three simulations, trial I-b for a single Aβ, trial II-c for two Aβs, and trial III-b for three Aβs, are connected to illustrate the movement of Aβs. The first, second, and third Aβ peptides are depicted in magenta, red, and orange, respectively. (b) Change in the z-axis of the center of mass of the Aβ peptide and those of the uppermost and lowermost atoms. The changes for the first, second, and third Aβs are shown in magenta, red, and orange, respectively. The centers of masses of GM1 head groups at the upper and lower leaflets are shown in green. (c) Binding free energy between Aβ peptides. The energies between the first and second Aβs, between the first and third Aβs, and between the second and third Aβs are colored in red, orange, and blue, respectively.

II-c. After 200 ns MD simulation, the third Aβ was bound to the membrane in both trials (Figure S7, Supporting Information). In trial III-a, the third Aβ was attached to the same side of the membrane as the second one, and the third Aβ made contact with the second one. The first Aβ was steadily attached to the membrane during the simulation (Figure S8, Supporting Information). Accordingly, the first Aβ peptide was not detached from the membrane for more than 300 ns, measured from the last point of trial I-b. In trial III-b, the third Aβ was attached to the opposite side to the first and second Aβs. In the course of a 200 ns simulation, the complex of the first and second Aβs was detached from the membrane and then moved to the opposite side.

dx.doi.org/10.1021/jp4029062 | J. Phys. Chem. B 2013, 117, 8085–8094

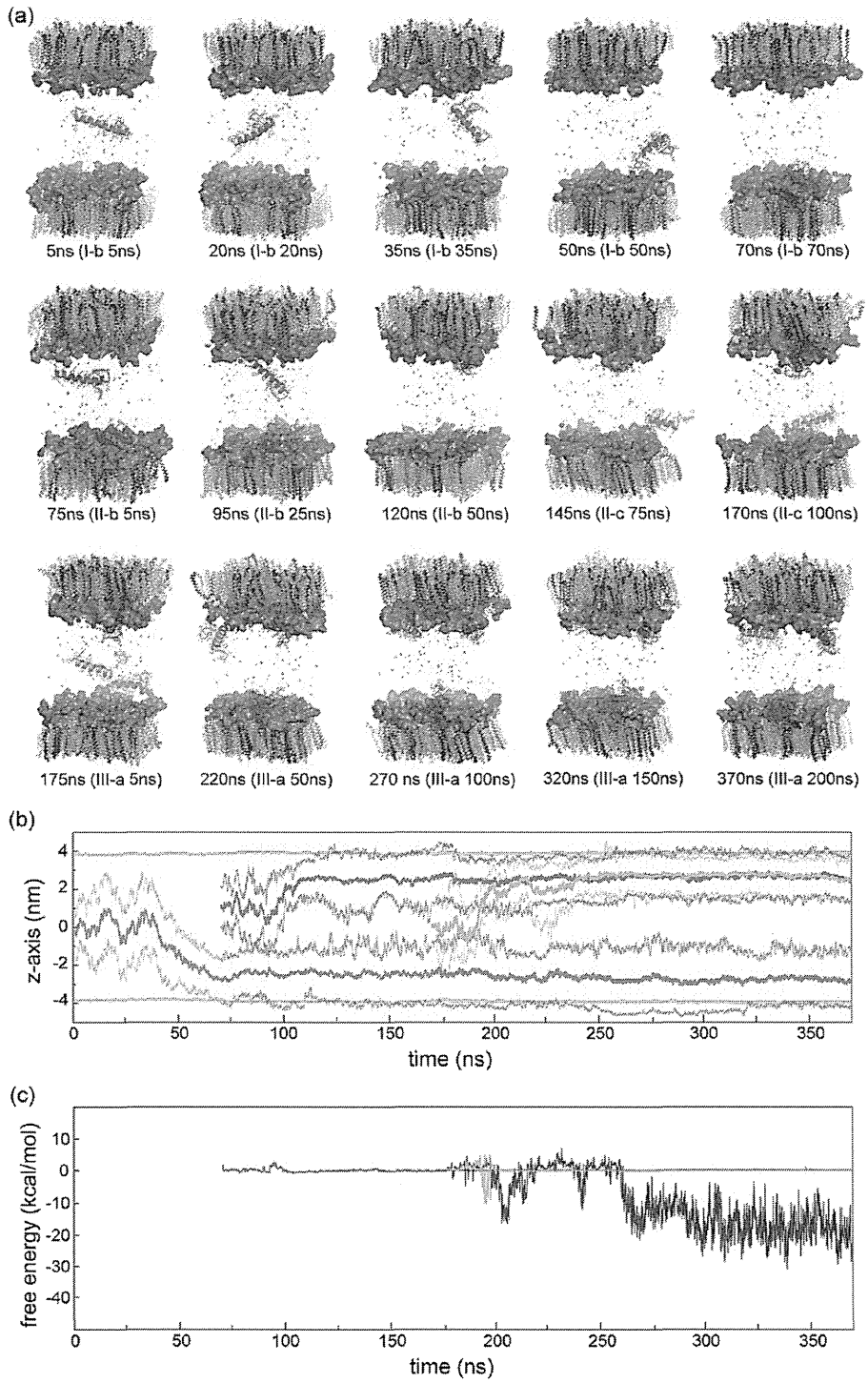

Figure 3. (a) Motion of the Aβ peptide in another calculation trial from Figure 2. Three simulations, trial I-b for a single Aβ, trial II-b for two Aβs, and trial III-a for three Aβs, are connected. The first, second, and third Aβ peptides are depicted in magenta, red, and orange, respectively. Since the simulation model is under a periodic boundary condition, the cell edge is connected to the corresponding opposite edge in the x, y, or z direction. Hence, the third Aβ was located at the vicinity of the second one and established contact of Aβ peptides after 270 ns, although the two Aβs are seen to be separated. (b) Change in the z-axis of the center of mass of the Aβ peptide and those of the uppermost and lowermost atoms. (c) Binding free energy between Aβ peptides. The color representation is the same as that in Figures 2(b) and (c).

Consequently, three Aβ peptides were located at the same side of the membrane and clustered together.

Interaction of Aβ Peptides. A typical motion of the Aβ_{1-42} peptide on the GM1-containing membrane is presented in Figure 2(a). Aβ initially fluctuated in the water layer and finally established close contact with the membrane at 70 ns. The second Aβ was added at the bulk water layer. The C-terminal side of the second Aβ was involved in the interaction with the first one. The interaction between C-terminal sides of both the second and first Aβs kept the second Aβ in the vicinity of the membrane for a long time. Finally, the second Aβ also established close contact with the membrane at 145 ns. Consequently, two

dx.doi.org/10.1021/jp4029062 | J. Phys. Chem. B 2013, 117, 8085–8094

Aβ peptides were attached to the lipid membrane with connection through their C-terminal regions. The third Aβ was added at the bulk water layer. The third Aβ was bound to the opposite leaflet of the membrane at 220 ns. The complex of the first and second Aβs was incidentally detached from the membrane and fluctuated in the water layer at 270 ns. The complex was bound to the opposite leaflet at 320 ns, which led to the interaction with the third Aβ. Consequently, the three Aβ peptides started to form a bundle on the GM1-containing lipid membrane. The change in z-axis coordinate of the center of mass for each Aβ peptide was monitored during MD simulation (Figure 2(b)), which clearly indicates the motions of Aβs described above.

Figure 2(c) shows the changes in binding free energies among Aβ peptides. The binding energy between the first and second Aβs was moderate for a while, but the energy gradually became lower. When the complex of the first Aβ and the second one was detached from the membrane at 270 ns, the binding energy was further lowered, and the complex of the first and second Aβs became quite stable. This drastic energy lowering was due to an increase in the area of hydrophobic contact between C-terminal regions of the two Aβ peptides. When the complex is bound to the membrane, conformational changes of both Aβs are restricted. In contrast, diverse conformational change becomes possible when the peptide complex is in the water layer. The binding energy between the first and third Aβs was moderate initially, but it was gradually lowered with the progress of MD simulation. It is notable that the interaction between the first and second Aβs was further enhanced with lowering of the binding energy between the first and third Aβs.

Another example of the motions of $A\beta_{1-42}$ peptides on the GM1-containing membrane is shown in Figure 3(a). The second Aβ added in the bulk water layer was eventually bound to the opposite leaflet of the membrane to that to which the first one was attached. The third Aβ first interacted with the first one, but it soon moved to the leaflet to which the second Aβ was attached. The third Aβ migrated on the membrane for a while and finally established close contact with the second one. It should be noted that the first Aβ was bound to the same leaflet throughout the simulation after it was bound to the membrane. The change in z-axis coordinate of the center of mass for each Aβ peptide was monitored (Figure 3(b)), and the changes in binding free energies among Aβ peptides were measured (Figure 3(c)). The binding energy between the first and second Aβs and that between the first and third Aβs were almost zero during the simulation. On the other hand, the binding energy between the second and third Aβs became lower due to their interaction. When the third Aβ was bound to the membrane at 220 ns, the binding energy was hardly lowered because the third Aβ had no contact with the second one, but it was gradually lowered with the progress of MD simulation after 260 ns. It is notable that the binding energy was almost the same value as that measured for the interaction between the first and second Aβs in the case shown in the previous example of Figure 2(c). That is, the strength of the initial interaction between two Aβ peptides on the membrane is consistent among the calculation trials.

DISCUSSION

Secondary Structure of Aβ Peptides. Aβ peptides aggregate into insoluble filamentous fibrils, which accumulate to become toxic plaques, eventually leading to the neurodegeneration.[35] A solution NMR study demonstrated that Aβ fibrils consisted of β-sheet peptides and that these β-sheet peptides were aligned to make a close packing.[36] Since the major content of a single isolated Aβ is an α-helix,[24,25] conformational transformation of the secondary structure of Aβ due to interaction with the lipid mixed membrane and/or another Aβ is of great interest. The change of the secondary structure was examined for the respective residues through MD simulations (Figures S9–S11, Supporting Information).

When a single $A\beta_{1-42}$ is bound to the lipid membrane, the α-helical content is slightly decreased. A typical example of decrease in the α-helical content can be seen in trial I-b (Figure S9, Supporting Information). The α-helix structures were limited to the region of residues 10–23. Turn or bend structures were increased with a decrease in α-helix content. The helix of the Aβ peptide often became loose in the water layer and showed the so-called π-helix structure in trials I-c, I-d, I-e, I-g, and I-j. In these trials, the α-helical region became straight compared to the initial structure. It is notable that an antiparallel β-sheet structure temporarily appeared at the C-terminal region in trials I-a, I-c, I-d, and I-e.

In the calculation for the model with two Aβs, there was almost no change in the secondary structure of the first Aβ peptide during the simulation (Figure S10, Supporting Information). The α-helix content of the second Aβ decreased, and a π-helix structure was observed in trials II-a and II-c. It should be noted that an antiparallel β-sheet structure sometimes appeared at the C-terminal region. In the calculations for the model with three Aβs, the first Aβ peptide showed no marked change in secondary structure (Figure S11, Supporting Information). A β-sheet structure appeared at the C-terminal regions of the second and third Aβs in both trials. A bend structure appeared at the regions around residue 26 in the second Aβ in trial III-a and in the third Aβ peptide in trial III-b. Consequently, it is concluded that the α-helical content of the Aβ peptide decreases due to binding to the membrane, and the unfolded helical region is barely recovered.

Interaction between the Aβ Peptide and GM1-Ganglioside. Aβ peptides showed Brownian motion in the water layer. Therefore, the amino acid residues of Aβ that first make contact with the membrane are at random. In 70 ns MD simulations for a single Aβ model, Aβ was firmly bound to the membrane in four trials. The hydrogen bonds between Aβ and GM1 oligosaccharide were monitored for the last 10 ns in all of these four trials (Table S2, Supporting Information). There was no predominant residue of Aβ for the initial contact between Aβ and the membrane. This hydrogen bond analysis suggests that no amino acid residue is regularly responsible for the initial binding of Aβ.

The importance of the CH–π stacking interaction between the galactose ring of ganglioside and the aromatic side chains of Aβ was previously pointed out by Tahi et al.[37] Indeed, π–π, CH–π, and OH–π interactions are deeply involved in protein folding and molecular recognition.[38,39] Hence, the distances from the aromatic rings of Phe4, Tyr10, Phe19, and Phe20 to the closest heavy atom of GM1 head groups were monitored for the last 10 ns of the MD simulation for the four trials (Figure S12, Supporting Information). In every trial, some aromatic rings were within a distance that enabled CH–π and/or OH–π stacking interaction with GM1. Accordingly, the CH–π and/or OH–π stacking interaction with GM1 oligosaccharide is concluded to be effective to keep Aβ peptides attached to the membrane surface. A previous study using the fluorescence titration technique suggested that nonelectrostatic interaction between Aβ and glycolipids was a driving factor for Aβ binding to the membrane.[40] Our simulation results are consistent with this

experimental finding. A typical structure for the CH−π interaction is shown in Figure 4(a).

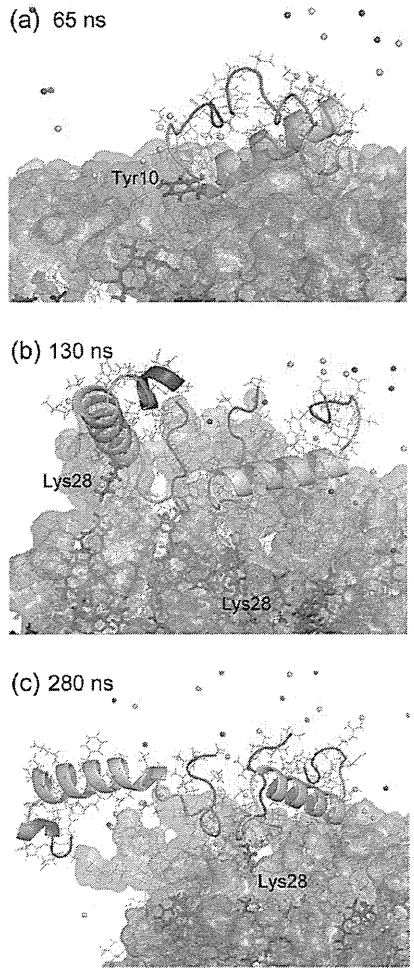

Figure 4. (a) Marked interactions of Aβ peptides on the GM1-clustering membrane. GM1 head groups are transparently depicted in light blue, but Neu5Ac's are shown in white. Main-chain atoms of Aβ peptides are colored in rainbow, where the color change from blue to red corresponds to the residue position from the N-terminus to C-terminus. Other representations are the same as those in Figure 1. Structures, (a), (b), and (c), are extracted from trials I-b, II-c, and III-b at the corresponding time in Figure 2.

A marked interaction involving strong binding of Aβ to GM1 clusters appeared in the progress of MD simulation after Aβ adhesion to the membrane. A typical structure for the strong interaction is shown in Figure 4(b), which was extracted from trial II-c at 130 ns measured from the beginning of the single Aβ simulation. Because of the clustering of GM1 head groups, some Neu5Ac residues gather at a local area of membrane surface, generating highly negatively charged regions. These regions present a characteristic environment like a pit on the membrane surface. The amine group on the side chain of Lys28 of Aβ was strongly trapped inside this Neu5Ac gathering pit. Due to the trapping of the Lys28 side chain, the area of residues 29−32 converted to a strand form. The C-terminal side of Aβ, residues 29−42, has high hydrophobicity. Owing to the conversion of residues 29−32 into the strand form, many hydrophobic residues at the C-terminal region were exposed to the solvent without forming any secondary structure and with hardly keeping intramolecular interaction. Hence, the C-terminal region was quite reactive to make hydrophobic contact with other molecules. Accordingly, the first Aβ had many chances for a strong hydrophobic interaction with the second one. The hydrophobic contact between the C-terminal regions of the first and second Aβs resulted in a more stable complex as shown in Figure 4(c). The C-terminal amino acid residues of both Aβ peptides were aligned and developed into a parallel β-sheet formation. This formation is a trigger for Aβ aggregation on the membrane.

It should be noted that amyloid fibrils have been suggested by experiments to have an antiparallel β-sheet structure.[41] In our simulation, the hydrophobic interaction of two Aβs was sometimes observed to start from the parallel β-sheet formation. When Aβ was bound to the membrane, the C-terminal region was often exposed to the solvent, and the C-terminal end was observed to swing ceaselessly. Hence, residues other than those of the terminal end are more likely to make initial hydrophobic contact when two Aβs approach each other. Accordingly, the C-terminal regions are likely to be aligned, and a parallel β-sheet structure will be favorably formed. A parallel β-sheet is, however, less stable than an antiparallel β-sheet because the hydrogen bonds making the parallel sheet are distorted in comparison to those for an antiparallel sheet. Therefore, an antiparallel sheet structure will be more dominant with the growth of amyloid fibrils.

Three characteristic structures shown in Figure 4 were also observed in another series of MD simulations (Figure S13, Supporting Information). Illustrations of the CH−π stacking interaction, trapping of the side chain of Lys28, and β-sheet formation of two Aβs were extracted from the snapshot structures at 40 and 95 ns of trial II-b and 145 ns of trial III-a, respectively. These structures will be valuable information to search for chemicals to block Aβ binding to the lipid membrane or to reduce Aβ fibril formation.

Comparison with Findings from Previous Studies. Some experimental studies have suggested that the Aβ peptide was bound to the GM1/SM/Chol mixed membrane in an α-helical formation when the molar ratio of Aβ to GM1 was low, but when the ratio was high, a β-strand-rich formation became dominant.[10,11] In our calculation, drastic transformation from α-helical to β-sheet structure was scarcely observed for a single Aβ even if it was bound to the GM1-containing membrane (Figure S9, Supporting Information). A β-sheet conformation sometimes appeared at the C-terminal region (Figure S10, Supporting Information), and the appearance continued for a long time when an Aβ made contact with another Aβ (Figure S11, Supporting Information). Hence, our results are consistent with the previous findings in that the concentration of Aβ is a key factor to promote the transformation into a β-sheet structure. In the simulations with a single Aβ model, the α-helical region sometime became straight compared to the initial structure as seen in trials I-b and I-c, which is one of the possible reasons for the increase in α-helical content experimentally observed in the early stage of Aβ binding to the lipid membrane.[11]

Several experimental studies have revealed the importance of the quantity of Neu5Acs for Aβ binding to ganglioside-containing membranes.[1,12] It is important to note that Aβ is barely bound to the mixed membrane consisting of GM1 and POPC even if Neu5Ac residues exist on the membrane surface.[10,11] A critical difference in GM1 formation between GM1/SM/Chol and GM1/POPC membranes is that GM1 gangliosides compose clusters only on the GM1/SM/Chol membrane. Due to the cluster formation, some Neu5Ac residues

come close to each other. The side chain of the basic amino acid residue, Lys28, is likely to be trapped by the gathering of these Neu5Acs. This finding explains why Aβ is favorably bound to the GM1/SM/Chol membrane.

Zhao et al. performed MD simulation of Aβ oligomers closely packed in the β-sheet formation at 398 K to observe the dissociation process of the packing form.[14] By monitoring the robustness to keep the β-sheet formation, they suggested that the hydrophobic segment at around Met35 was a key region for maintaining the structural stability of Aβ oligomers. They further proposed that the hydrophobic segment was a nucleation site for Aβ aggregation. In our simulation, Aβ dimerization was observed to start with hydrophobic contact at the region around Met35, which is compatible with the above suggestion. An important role of the hydrophobic contact for Aβ aggregation has been commonly observed in some previous studies.[15−17]

Through MD simulation, Davis et al. performed an energetic analysis of the process of Aβ binding to a lipid membrane and subsequent dimerization.[21] They calculated the stabilization energy for the process to be −20 to −46 kcal/mol. The present study demonstrated that the interaction energy of two Aβs was gradually decreased with the evolution of Aβ dimer formation and consequently reached about −40 kcal/mol. This energy is comparable with the value calculated in the above study. It is interesting to note that these calculated energies are of a degree of affinity similar to the stable peptide−protein interaction as seen in the epitope recognition by human leukocyte antigen.[42]

It was reported that nanoparticles consisting of isopropylacrylamide enhanced the rate of the formation of Aβ fibrils, while copolymeric particles of isopropylacrylamide and butylacrylamide retarded Aβ fibrillation.[43] Nanoparticles were suggested to be mainly involved in the nucleation step of the Aβ fibrillation process because, once Aβ nuclei were generated, the subsequent fibril elongation was scarcely affected by the presence of the particles. The rate of Aβ fibrillation was dominantly influenced by the component of polymers comprising the nanoparticles and also by their concentration in buffer solution.[44,45] The nanoparticle-induced fibril enhancement was suggested to be due to the hydrophobic character of the surface.[43] That is, the particles provide a more hydrophobic environment than water. In this regard, it is interesting that toxic Aβ aggregation occurs without any surface like a membrane or particle if the polarity or dielectricity of the buffer is well controlled.[41,46] The existence of some kinds of surfaces such as nanoparticles or membranes will be a secondary factor to enhance Aβ fibril formation. In the case of nanoparticle-mediated fibrillation, it was proposed that hydrogen bonds were formed between the particle polymer backbone and the polar groups of the peptide.[44] In our simulation, a certain number of hydrogen bonds were observed between the membrane surface and Aβ peptides. Therefore, nanoparticles are considered to have a role essentially similar to that of the GM1-containing membrane so that both nanoparticles and membranes serve as platforms to provide an adequate environment for Aβ peptides to cause nucleation and subsequent growth of fibrils.

Adhesion of the Histidine-Protonated Aβ Peptide on a GM1-Containing Membrane. Several studies have shown that a membrane-binding peptide was attracted to acidic lipids on a membrane by electrostatic force.[47,48] The influence of the charge of the membrane on Aβ was analyzed in some works.[19,49,50] However, it should be noted that the Aβ peptide is specifically bound to the ganglioside-containing membrane under physiological ionic strength and at neutral pH.[12] The effect of negative charge on the membrane surface is usually weakened by the presence of ions and solvent. To examine the influence of electrostatic interaction on Aβ binding, we carried out additional 60 ns MD simulations with the Aβ peptide set to be in a different charge state, in which the three residues His6, His13, and His14 were protonated. The final conformations for five trials of the 60 ns MD simulations are shown in Figure S14 (Supporting Information), and changes in the z-axis and secondary structure of the Aβ peptide were monitored (Figures S15 and S16, Supporting Information). A comparison with the single Aβ simulation in Figures S3, S4, and S9 (Supporting Information) indicates that there is no drastic change in the motion of Aβ peptides, while the binding probability was increased to some extent. Therefore, the charge state of the Aβ peptide is not essentially important for binding, and the negative charge of Neu5Ac is not the driving force to attract Aβs to the GM1-containing membrane. Instead, the electrostatic interaction is effective for stably maintaining Aβ binding once Aβ is trapped on the membrane surface.

CONCLUSION

Multiple MD simulations demonstrated that Aβ peptide was capable of being attached to the GM1-containing membrane, in which CH−π and OH−π interactions between the aromatic rings of Aβ side chains and GM1 oligosaccharides assisted the Aβ adhesion. Aβ was further tightly bound to the lipid membrane when the amine group of Lys28 was held by the Neu5Ac gathering pit on the GM1 cluster. The amine group worked as an anchor to strongly link the Aβ peptide to the membrane surface. When the second Aβ approached the first Aβ, the two Aβ peptides made a complex. Hydrophobic contact was generated between the C-terminal regions of these two Aβ peptides. Holding of Lys28 by Neu5Ac residues on the GM1 cluster assisted the formation of hydrophobic contact because the secondary structure was hardly maintained at the C-terminal region and the hydrophobic area was exposed to the solvent. The contact between the C-terminal regions of the two Aβs resulted in the formation of a parallel β-sheet structure. The third Aβ peptide was observed to be bound to the complex of the two Aβ peptides to make a bundle of Aβ peptides. The strong hydrophobic interaction between two Aβ peptides occasionally induced detachment of the Aβ peptide complex.

ASSOCIATED CONTENT

Supporting Information

Cluster analysis of Aβ peptides, hydrogen-bond interaction, time courses of the MD simulations, final structures of the simulations, change of z-axis of the Aβ peptide, change of the secondary structure, marked interaction of Aβ peptide with membrane, and results for the positively charged Aβ peptide. This material is available free of charge via the Internet at http://pubs.acs.org.

AUTHOR INFORMATION

Corresponding Author

*Phone: +81-43-226-2936. Fax: +81-43-226-2936. E-mail: hoshino@chiba-u.jp.

Present Address

⊥Chemistry Research Labs, Drug Discovery Research, Astellas Pharma Inc.

Notes

The authors declare no competing financial interest.

■ ACKNOWLEDGMENTS

Calculations were performed at Research Center for Computational Science, Okazaki, Japan, and at Information Technology Center of the University of Tokyo. A part of this work was supported by a grant for Scientific Research C from the Japan Society for the Promotion of Science and a Grant-in-Aid from the Ministry of Health and Labor of Japan. This work was also supported in part by The Research Funding for Longevity Sciences (22-14 and 25-19) from National Center for Geriatrics and Gerontology (NCGG), Japan.

■ REFERENCES

(1) McLaurin, J.; Franklin, T.; Fraser, P.; Chakrabartty, A. Structural Transitions Associated with the Interaction of Alzheimer Beta-Amyloid Peptides with Gangliosides. *J. Biol. Chem.* **1998**, *273*, 4506−4515 and references therein.

(2) Haass, C.; Selkoe, D. J. Soluble Protein Oligomers in Neurodegeneration: Lessons from the Alzheimer's Amyloid Beta-Peptide. *Nat. Rev. Mol. Cell. Biol.* **2007**, *8*, 101−112 and references therein.

(3) Citron, M.; Vigo-Pelfrey, C.; Teplow, D. B.; Miller, C.; Schenk, D.; Johnston, J.; Winblad, B.; Venizelos, N.; Lannfelt, L.; Selkoe, D. J. Excessive Production of Amyloid Beta-Protein by Peripheral Cells of Symptomatic and Presymptomatic Patients Carrying the Swedish Familial Alzheimer Disease Mutation. *Proc. Natl. Acad. Sci. U.S.A.* **1994**, *91*, 11993−11997.

(4) Torok, M.; Milton, S.; Kayed, R.; Wu, P.; McIntire, T.; Glabe, C. G.; Langen, R. Structural and Dynamic Features of Alzheimer's Aβ Peptide in Amyloid Fibrils Studied by Site-Directed Spin Labeling. *J. Biol. Chem.* **2002**, *277*, 40810−40815.

(5) Ogawa, M.; Tsukuda, M.; Yamaguchi, T.; Ikeda, K.; Okada, T.; Yano, Y.; Hoshino, M.; Matsuzaki, K. Ganglioside-Mediated Aggregation of Amyloid β-Proteins (Aβ): Comparison between Aβ-(1−40) and Aβ-(1−42). *J. Neurochem.* **2011**, *116*, 851−857.

(6) Choo-Smith, L. P.; Surewicz, W. K. The Interaction between Alzheimer Amyloid Beta(1−40) Peptide and Ganglioside GM1-Containing Membranes. *FEBS Lett.* **1997**, *402*, 95−98.

(7) Ariga, T.; Kobayashi, K.; Hasegawa, A.; Kiso, M.; Ishida, H.; Miyatake, T. Characterization of High-Affinity Binding between Gangliosides and Amyloid Beta-Protein. *Arch. Biochem. Biophys.* **2001**, *388*, 225−230.

(8) Hayashi, H.; Kimura, N.; Yamaguchi, H.; Hasegawa, K.; Yokoseki, T.; Shibata, M.; Yamamoto, N.; Michikawa, M.; Yoshikawa, Y.; Terao, K.; Matsuzaki, K.; Lemere, C. A.; Selkoe, D. J.; Naiki, H.; Yanagisawa, K. A Seed for Alzheimer Amyloid in the Brain. *J. Neurosci.* **2004**, *24*, 4894−4902.

(9) Yanagisawa, K.; Odaka, A.; Suzuki, N.; Ihara, Y. GM1 Ganglioside-Bound Amyloid β-Protein (Aβ): A Possible Form of Preamyloid in Alzheimer's Disease. *Nat. Med.* **1995**, *1*, 1062−1066.

(10) Kakio, A.; Nishimoto, S.; Yanagisawa, K.; Kozutsumi, Y.; Matsuzaki, K. Cholesterol-Dependent Formation of GM1 Ganglioside-Bound Amyloid β-Protein, An Endogenous Seed for Alzheimer Amyloid. *J. Biol. Chem.* **2001**, *276*, 24985−24990.

(11) Kakio, A.; Nishimoto, S.; Yanagisawa, K.; Kozutsumi, Y.; Matsuzaki, K. Interactions of Amyloid Beta-Protein with Various Gangliosides in Raft-Like Membranes: Importance of GM1 Ganglioside-Bound Form as an Andogenous Seed for Alzheimer Amyloid. *Biochemistry* **2002**, *41*, 7385−7390.

(12) Matsuzaki, K.; Horikiri, C. Interactions of Amyloid β-Peptide (1−40) with Ganglioside-Containing Membranes. *Biochemistry* **1999**, *38*, 4137−4142.

(13) Mori, K.; Mahmood, M. I.; Neya, S.; Matsuzaki, K.; Hoshino, T. Formation of GM1 Ganglioside Clusters on the Lipid Membrane Containing Sphingomyeline and Cholesterol. *J. Phys. Chem. B* **2012**, *116*, 5111−5121.

(14) Zhao, J. H.; Liu, H. L.; Liu, Y. F.; Lin, H. Y.; Fang, H. W.; Ho, Y.; Tsai, W. B. Molecular Dynamics Simulations to Investigate the Aggregation Behavior of the Aβ(17−42) Oligomers. *J. Biomol. Struct. Dyn.* **2009**, *26*, 481−490.

(15) Zhu, X.; Bora, R. P.; Barman, A.; Singh, R.; Prabhakar, R. Dimerization of the Full-Length Alzheimer Amyloid β-Peptide (Aβ42) in Explicit Aqueous Solution: a Molecular Dynamics Study. *J. Phys. Chem. B* **2012**, *116*, 4405−4416.

(16) Chong, S. H.; Ham, S. Impact of Chemical Heterogeneity on Protein Self-Assembly in Water. *Proc. Natl. Acad. Sci. U.S.A.* **2012**, *109*, 7636−7641.

(17) Barz, B.; Urbanc, B. Dimer Formation Enhances Structural Differences between Amyloid β-Protein (1−40) and (1−42): An Explicit-Solvent Molecular Dynamics Study. *PLoS One* **2012**, *7*, e34345.

(18) Xu, Y.; Shen, J.; Luo, X.; Zhu, W.; Chen, K.; Ma, J.; Jiang, H. Conformational Transition of Amyloid Beta-Peptide. *Proc. Natl. Acad. Sci. U.S.A.* **2005**, *102*, 5403−5407.

(19) Tofoleanu, F.; Buchete, N. V. Molecular Interactions of Alzheimer's Aβ Protofilaments with Lipid Membranes. *J. Mol. Biol.* **2012**, *421*, 572−586.

(20) Davis, C. H.; Berkowitz, M. L. Structure of the Amyloid-Beta (1−42) Monomer Absorbed to Model Phospholipid Bilayers: A Molecular Dynamics Study. *J. Phys. Chem. B* **2009**, *113*, 14480−14486.

(21) Davis, C. H.; Berkowitz, M. L. A Molecular Dynamics Study of the Early Stages of Amyloid-Beta(1−42) Oligomerization: The Role of Lipid Membranes. *Proteins* **2010**, *78*, 2533−2545.

(22) Yu, X.; Zheng, J. Cholesterol Promotes the Interaction of Alzheimer β-Amyloid Monomer with Lipid Bilayer. *J. Mol. Biol.* **2012**, *421*, 561−571.

(23) Zhao, L. N.; Chiu, S. W.; Benoit, J.; Chew, L. Y.; Mu, Y. Amyloid β Peptides Aggregation in a Mixed Membrane Bilayer: A Molecular Dynamics Study. *J. Phys. Chem. B* **2011**, *115*, 12247−12256.

(24) Tomaselli, S.; Esposito, V.; Vangone, P.; van Nuland, N. A.; Bonvin, A. M.; Guerrini, R.; Tancredi, T.; Temussi, P. A.; Picone, D. The Alpha-to-Beta Conformational Transition of Alzheimer's Aβ-(1−42) Peptide in Aqueous Media is Reversible: A Step by Step Conformational Analysis Suggests the Location of Beta Conformation Seeding. *ChemBioChem* **2006**, *7*, 257−267.

(25) Crescenzi, O.; Tomaselli, S.; Guerrini, R.; Salvadori, S.; D'Ursi, A. M.; Temussi, P. A.; Picone, D. Solution Structure of the Alzheimer Amyloid Beta-Peptide (1−42) in an Apolar Microenvironment. Similarity with a Virus Fusion Domain. *Eur. J. Biochem.* **2002**, *269*, 5642−5648.

(26) Phillips, J. C.; Braun, R.; Wang, W.; Gumbart, J.; Tajkhorshid, E.; Villa, E.; Chipot, C.; Skeel, R. D.; Kale, L.; Schulten, K. Scalable Molecular Dynamics with NAMD. *J. Comput. Chem.* **2005**, *26*, 1781−1802.

(27) Mori, K.; Hata, M.; Neya, S.; Hoshino, T. MD Simulation of Asymmetric Phospholipid Bilayers with Ions and Cholesterols. *Chem-Bio Inf. J.* **2004**, *4*, 15−26.

(28) Yanagita, H.; Yamamoto, N.; Fuji, H.; Liu, X. L.; Ogata, M.; Yokota, M.; Takaku, H.; Hasegawa, H.; Odagiri, T.; Tashiro, M.; Hoshino, T. Mechanism of Drug Resistance of Hemagglutinin of Influenza Virus and Potent Scaffolds Inhibiting its Function. *ACS Chem. Biol.* **2012**, *7*, 552−562.

(29) Humphrey, W.; Dalke, A.; Schulten, K. VMD - Visual Molecular Dynamics. *J. Mol. Graphics* **1996**, *14*, 33−38.

(30) Case, D. A.; Cheatham, T. E., III; Darden, T.; Gohlke, H.; Luo, R.; Merz, K .M., Jr.; Onufriev, A.; Simmerling, C.; Wang, B.; Woods, R. The Amber Biomolecular Simulation Programs. *J. Computat. Chem.* **2005**, *26*, 1668−1688.

(31) Matsuyama, S.; Aydan, A.; Ode, H.; Hata, M.; Sugiura, W.; Hoshino, T. Structural and Energetic Analysis on the Complexes of Clinically-Isolated Subtype C HIV-1 Proteases and Approved Inhibitors by Molecular Dynamics Simulation. *J. Phys. Chem. B* **2010**, *114*, 521−530.

(32) Sano, E.; Li, W.; Yuki, H.; Liu, X.; Furihata, T.; Kobayashi, K.; Chiba, K.; Neya, S.; Hoshino, T. Mechanism of the Decrease in Catalytic Activity of Human Cytochrome P450 2C9 Polymorphic Variants, Investigated by Computational Analysis. *J. Comput. Chem.* **2010**, *31*, 2746−2758.

(33) Kabsch, W.; Sander, C. Dictionary of Protein Secondary Structure: Pattern Recognition of Hydrogen-bonded and Geometrical Features. *Biopolymers* **1983**, *22*, 2577−2637.
(34) DeLano, W. L. *The PyMOL Molecular Graphics System*; Schrödinger, LLC.
(35) Rochet, J. C.; Lansbury, P. T., Jr. Amyloid Fibrillogenesis: Themes and Variations. *Curr. Opin. Struct. Biol.* **2000**, *10*, 60−68.
(36) Hou, L.; Kang, I.; Marchant, R. E.; Zagorski, M. G. Methionine 35 Oxidation Reduces Fibril Assembly of the Amyloid Aβ-(1−42) Peptide of Alzheimer's Disease. *J. Biol. Chem.* **2002**, *277*, 40173−40176.
(37) Yahi, N.; Aulas, A.; Fantini, J. How Cholesterol Constrains Glycolipid Conformation for Optimal Recognition of Alzheimer's β Amyloid Peptide ($A\beta_{1-40}$). *PLos One* **2010**, *5*, e9079.
(38) Yuki, H.; Tanaka, Y.; Hata, M.; Ishikawa, H.; Neya, S.; Hoshino, T. Implementation of π-π Interactions in Molecular Dynamics Simulation. *J. Comput. Chem.* **2007**, *28*, 1091−1099.
(39) Ozawa, T.; Okazaki, K.; Kitaura, K. Importance of CH/π Hydrogen Bonds in Recognition of the Core Motif in Proline-Recognition Domains: An Ab Initio Fragment Molecular Orbital Study. *J. Comput. Chem.* **2011**, *32*, 2774−2782.
(40) Ikeda, K.; Matsuzaki, K. Driving Force of Binding of Amyloid Beta-Protein to Lipid Bilayers. *Biochem. Biophys. Res. Commun.* **2008**, *370*, 525−529.
(41) Fukunaga, S.; Ueno, H.; Yamaguchi, T.; Yano, Y.; Hoshino, M.; Matsuzaki, K. GM1 Cluster Mediates Formation of Toxic Aβ Fibrils by Providing Hydrophobic Environments. *Biochemistry* **2012**, *51*, 8125−8131.
(42) Mahmood, M. I.; Matsuo, Y.; Neya, S.; Hoshino, T. Computational Analysis on the Binding of Epitope Peptide to Human Leukocyte Antigen Class I Molecule A*2402 Subtype. *Chem. Pharm. Bull.* **2011**, *59*, 1254−1262.
(43) Colvin, V. L.; Kulinowski, K. M. Nanoparticles as Catalysts for Protein Fibrillation. *Proc. Natl. Acad. Sci. U.S.A.* **2007**, *104*, 8679−8680.
(44) Cabaleiro-Lago, C.; Quinlan-Pluck, F.; Lynch, I.; Lindman, S.; Minogue, A. M.; Thulin, E.; Walsh, D. M.; Dawson, K. A.; Linse, S. Inhibition of Amyloid β Protein Fibrillation by Polymeric Nanoparticles. *J. Am. Chem. Soc.* **2008**, *130*, 15437−15443.
(45) Cabaleiro-Lago, C.; Quinlan-Pluck, F.; Lynch, I.; Dawson, K. A.; Linse, S. Dual Effect of Amino Modified Polystyrene Nanoparticles on Amyloid β Protein Fibrillation. *ACS Chem. Neurosci.* **2010**, *1*, 279−287.
(46) Abedini, A.; Raleigh, D. P. A Critical Assessment of the Role of Helical Intermediates in Amyloid Formation by Natively Unfolded Proteins and Polypeptides. *Protein Eng., Des. Sel.* **2009**, *22*, 453−459.
(47) Ben-Tal, N.; Honig, B.; Miller, C.; McLaughlin, S. Electrostatic Binding of Proteins to Membranes. Theoretical Predictions and Experimental Results with Charybdotoxin and Phospholipid Vesicles. *Biophys. J.* **1997**, *73*, 1717−1727.
(48) Langner, M.; Kubica, K. The Electrostatics of Lipid Surfaces. *Chem. Phys. Lipids* **1999**, *101*, 3−35.
(49) Grimaldi, M.; Scrima, M.; Esposito, C.; Vitiello, G.; Ramunno, A.; Limongelli, V.; D'Errico, G.; Novellino, E.; D'Ursi, A. M. Membrane Charge Dependent States of the Beta-Amyloid Fragment Abeta (16−35) with Differently Charged Micelle Aggregates. *Biochim. Biophys. Acta* **2010**, *1798*, 660−761.
(50) Davis, C. H.; Berkowitz, M. L. Interaction Between Amyloid-β (1−42) Peptide and Phospholipid Bilayers: A Molecular Dynamics Study. *Biophys. J.* **2009**, *96*, 785−797.